Predictive Analytical Model of Fundamental Frequency and Imperfections in Glassblown Fused Quartz Hemi-toroidal 3D Micro Shells

Yusheng Wang, Mohammad H. Asadian, and Andrei M. Shkel
MicroSystems Laboratory
Department of Mechanical and Aerospace Engineering
University of California, Irvine, CA, 92697, USA
{yushengw, asadianm, andrei.shkel}@uci.edu

***Abstract*—Glassblown 3D micro shells are released by a multi-step mechanical lapping process, introducing structural imperfections to the sensing element. We present an analytical model predicting the frequency mismatch in micro shells due to imperfections induced by the release process. The analytical model of such micro shells was derived based on inextensional assumption. Mode shapes and the resonant frequencies were calculated and compared to results from both Finite Element Analysis (FEA) and experiments. The predictive frequency of the *n*=2 wineglass mode shape was within 10% of the finite element results and 20% of the experimental results for thin shells, showing the fidelity of the model. The effect of imperfections of the shell release process on frequency mismatch was studied both analytically and experimentally.**

Keywords—3D micro shell; MEMS; frequency mismatch; release by lapping; imperfection of release.

I. INTRODUCTION

Inspired by the performance of macro-scale Hemispherical Resonator Gyroscope (HRG) [1], there has been an increased interest in the development of 3D micro-scale resonators for vibratory inertial MEMS devices. Fused Quartz micro wineglass resonators [2] and micro birdbath shell resonators [3] have been fabricated by MEMS technology, demonstrating a potential of micro 3D structures, implemented by glassblowing, for exceptional symmetry, survivability to external vibrations, mechanical shock, and low energy losses. Wafer-scale MEMS fabrication of 3D structures, however, remains a challenge due to a necessary mechanical release step and a wafer-level assembly by bonding of released structures to an electrode wafer. The process of fabricating the 3D sensing element integrated with electrode is more difficult as compared to conventional micro-machining, which is limited to 2D architectures. However, the efforts to overcome the technological challenges of 3D shell micro-systems are well justified, as demonstrated devices are already exhibiting lower damping, frequency mismatches, and a potential for resistance to shock and vibration, opening a door of opportunities to high performance sensors, such as gyroscopes operating in rate integrating and mode-matched angular rate modes [4].

The frequency and frequency mismatch estimations of macro-machined hemispherical shells have been thoroughly studied in [5]. Micro-fabricated shells, however, take shapes closer to hemi-torus than hemi-sphere (Fig. 1). Directly applying the models developed for hemispherical shells to hemi-toroidal shells may lead to large errors (over 50% error for shells with comparable thickness and outer radius), and no models predicting the frequency of hemi-toroidal shells have been previously developed. This paper intends to fill this gap.

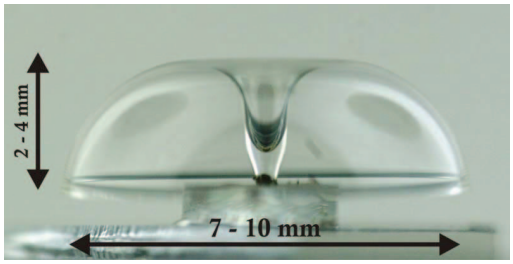

Fig. 1. Hemi-toroidal shell fabricated using high temperature micro-glassblowing process of Fused Quartz.

In this paper, an analytical model of hemi-toroidal shell was introduced based on inextensional wineglass mode shape assumption. Natural frequency of a perfect shell was derived by applying Rayleigh's energy method and verified experimentally. The response of shells with imperfections due to release was investigated analytically and experimentally.

II. ANALYTICAL MODEL

A. Derivation of Mode Shapes

Fig. 2 shows a thin hemi-toroidal shell with thickness h and radius R. In spherical coordinates, the shape of the shell can be expressed as $r=2R\sin\theta$, where r is the radial distance and θ is the polar angle. Since the shell is axisymmetric, r is independent of φ, and the latter is defined as the azimuth angle. The local displacement components are δr, $\delta\theta$, and $\delta\varphi$, where δr is the linear displacement along r, while $\delta\theta$ and $\delta\varphi$ are the angular displacement of θ and φ, respectively. In the wineglass mode, the displacement components are expressed as

$$\begin{aligned}\delta r &= U(\theta)\sin n\varphi\cos\omega t \\ \delta\theta &= V(\theta)\sin n\varphi\cos\omega t \\ \delta\varphi &= W(\theta)\cos n\varphi\cos\omega t\end{aligned} \quad \text{and} \quad \begin{aligned}\delta r &= U(\theta)\cos n\varphi\cos\omega t \\ \delta\theta &= V(\theta)\cos n\varphi\cos\omega t \\ \delta\varphi &= W(\theta)\sin n\varphi\cos\omega t\end{aligned} \qquad (1)$$

for two matched modes, where n is the mode number, ω is the angular frequency of the mode, and U, V, and W are mode

This material is based upon work supported by DARPA grant W31P4Q-11-1-0006 (Program Manager Dr. Robert Lutwak).

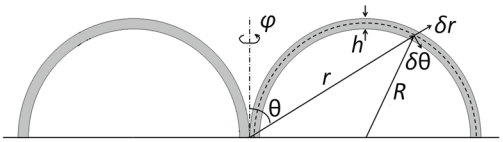

Fig. 2. Coordinate system, middle surface (dashed line) and parameters of hemi-toroidal shell.

shape functions of variable θ [6], and they are to be determined later in the paper. The terms in (1) containing φ define the orientation of the mode shape and the terms containing ω define the frequency.

Inextensional assumption is applied to calculate the mode shape, which means the strain of the middle surface of the shell remains zero during the deformation. This assumption holds if thickness of the shell is much smaller than the other dimensions [6]. In the case of glassblown structures, the thickness of the shell is on the order of 100μm, while the outer radius is on the order of 10mm and the height is about 3mm (Fig. 1). Hence, due to the ratio of dimensions, the inextensional assumption is justifiable to apply for the structures of interest. Movement of the shell structure is completely described by the movement of its middle surface.

Let us consider an arbitrary line element ds on the middle surface of the shell at position (r, θ, φ), with the length components of dr, $d\theta$, and $d\varphi$. After deformation of the shell, the coordinates of the element become $r+\delta r$, $\theta+\delta\theta$, and $\varphi+\delta\varphi$, respectively. The length of the line element can be expressed as

$$\begin{aligned}(ds+d\delta s)^2 = &(dr+d\delta r)^2 + \\ &(r+\delta r)^2\sin^2(\theta+\delta\theta)(d\varphi+d\delta\varphi)^2 + \\ &(r+\delta r)^2(d\theta+d\delta\theta)^2\end{aligned} \quad (2)$$

We expand the differential elements in displacement and geometry with respect to coordinates θ and φ as follows:

$$d\delta z = \frac{\partial\delta z}{\partial\theta}d\theta + \frac{\partial\delta z}{\partial\varphi}d\varphi,\ dr = \frac{dr}{d\theta}d\theta,$$

where z is the coordinate variable and it applies to r, θ, and φ.

Consider only the lowest order terms in (2). The resulting equation for the deformation of the line element takes the form:

$$\begin{aligned}\frac{d\delta s}{ds} = &\left(\frac{dr}{d\theta}\frac{\partial\delta r}{\partial\theta} + r^2\frac{\partial\delta\theta}{\partial\theta} + r\delta r\right)\frac{d\theta^2}{ds^2} + \\ &\left(r\delta r\sin^2\theta + r^2\sin\theta\cos\theta\delta\theta + r^2\frac{\partial\delta\varphi}{\partial\varphi}\sin^2\theta\right)\frac{d\varphi^2}{ds^2} + \\ &\left(\frac{dr}{d\theta}\frac{\partial\delta r}{\partial\varphi} + r^2\frac{\partial\delta\theta}{\partial\varphi} + r^2\frac{\partial\delta\varphi}{\partial\theta}\sin^2\theta\right)\frac{d\theta d\varphi}{ds^2}\end{aligned} \quad (3)$$

According to the inextensional assumption, the length after deformation should not change no matter what values dr, $d\theta$, and $d\varphi$ would take, which implies that the coefficients of all terms on the right hand side of (3) are zero.

Substituting (1) in (3) and canceling the two variables δr and $\delta\theta$ would cancel the common orientation term and the frequency term. The resulting fundamental equation of the mode shape of the hemi-toroidal shell will be

$$\left(\cos^2\theta - \sin^2\theta\right)\frac{d^2 r_\varphi}{d\theta^2} + 4\sin\theta\cos\theta\frac{dr_\varphi}{d\theta} + \frac{2n^2-1}{\sin^2\theta}r_\varphi = 0, \quad (4)$$

where $r_\varphi = r\,W(\theta)\sin\theta$ represents the linear displacement along the azimuth angle. We are solving for r_φ instead of $W(\theta)$ to avoid the singularity of the third term on the left hand side of (4), since r_φ is also second order infinitesimal when θ=0.

Equation (4) is a linear second-order ordinary differential equation with varying coefficients. Clamped boundary condition was assumed and collocation method was applied to solve the equation numerically [7]. Hermite polynomials of order three were used to approximate the solution. The solution is shown by the blue solid line in Fig. 3. The red dashed line in Fig. 3 is the normalized result from Finite Element Analysis; COMSOL Multiphysics was used for the FEA model. The largest error was about 1% of the maximum displacement, where θ was about 0.5rad. The small error indicates the fidelity of the developed analytical model.

B. Calculation of Resonant Frequency

Resonant frequency of the shell was derived by Rayleigh's energy method [5]. First, the kinetic energy K_0 and the strain energy U_0 of the shell were calculated based on the mode shape and arbitrary amplitude of motion A:

$$K_0 = \frac{1}{2}\rho\iiint_\Omega\left(\dot\delta r^2 + r^2\dot\delta\theta^2 + r^2\sin^2\theta\dot\delta\varphi^2\right)dV, \quad (5)$$

$$U_0 = \frac{1}{2}\iiint_\Omega\left(\sigma_{11}\varepsilon_{11} + \sigma_{22}\varepsilon_{22} + \sigma_{12}\varepsilon_{12}\right)dV, \quad (6)$$

where Ω is the integration region, which is the shape of the shell. Then, the Lagrangian was expressed as $L = U_{0\max} - K_{0\max}$, where $U_{0\max}$ and $K_{0\max}$ are the maximum of kinetic energy and strain energy, respectively. Finally, solving Rayleigh's equation $\partial L/\partial A = 0$ gave us the angular frequency of the shell.

As shown in Fig. 4, the analytical model matches well with the finite element model for the n=2 mode. The error is within 10% for the shell with thickness less than 400μm. Since inextensional assumption can only be applied to thin shells, larger errors for thicker shells are expected.

C. Calculation of Frequency Mismatch

The shell release is a step in the fabrication process where the substrate of glassblown structure is physically removed [2]. Mechanical lapping is the method used for release. Additional

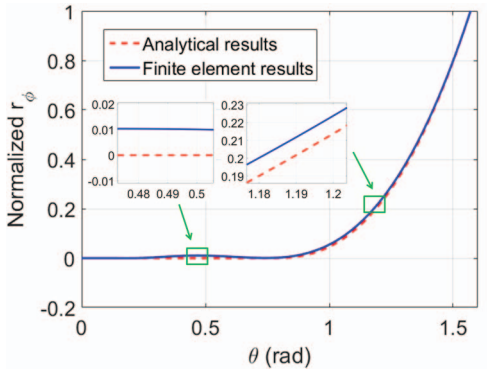

Fig. 3. Comparison of n=2 mode shapes from analytical model and finite element model. Displacements in φ direction are normalized.

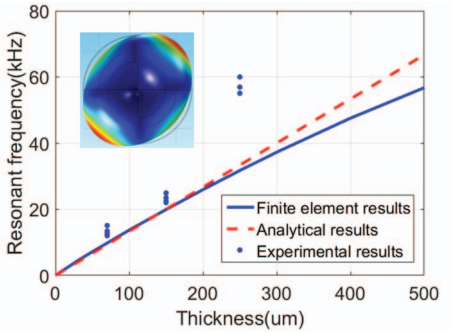

Fig. 4. Relation between resonant frequency of n=2 mode and the thickness of the shell.

frequency mismatch may be introduced if the lapping plane is not strictly vertical to the stem of the shell, Fig. 5 (a). This phenomenon is studied both analytically and experimentally.

The mode shape of a resonator can be considered unaffected by small shape disturbance [5]. Therefore, in this study we only have to change the integration regions in (5) and (6) from axisymmetric region to the actual shape of the shell, without recalculating the mode shape itself. The frequencies of two mode shapes will be different due to the asymmetric integration region. The relation between the angular lapping error (β) and the frequency mismatch is shown in Fig. 5 (a).

III. Experimental Results

A. Resonant Frequency

Frequencies of micro shells with outer diameter of 7mm and thickness of 70μm, 150μm, and 250μm were tested to verify the analytical model. The shells were actuated along the stem by piezoelectric element temperorily attached to the shell by Field's metal and characterized optically by Laser Doppler Vibrometer (LDV) in vacuum chamber under pressure on the order of 20μTorr. The results are presented in Fig. 4, showing the maximum errors of about 20%, when the shell thickness is less than 150μm. The errors are possibly due to non-uniformity of the thickness and over-release of shells. For thick shells, the errors are relatively large because the shells are not fully developed during glassblowing and the shape consequently deviates from hemi-torus.

B. Frequency Mismatch

Special lapping fixtures were designed and fabricated by 3D printing to release shells with specific lapping angle, Fig. 5 (b). The lapping fixtures were designed to create tilted angle of 1 degree. This allows the lapping angular error to increase 1 degree after each subsequent lapping. The micro-fabricated shells were first attached to a silicon die by Crystalbond 509-3. The silicon die was used as a reference plane coinciding with the edge of the shell. Then, the silicon die together with the shell was attached to the lapping fixture. The shell was cleaned and characterized after each asymmetric lapping.

The results shown in Fig. 5 (b) illustrate the predicted effect. The model confirms the trend of changes, however, experimental change of frequency mismatch increases faster than the model predicts. One possible reason might be the fact that the thickness of the rim of the shell is much larger than in

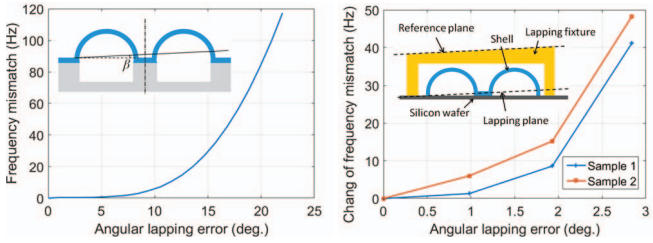

(a) (b)

Fig. 5. (a). Modeled relation between the lapping error (β) and frequency mismatch. (b). Experiment results of the relation between the lapping error and frequency mismatch.

other regions of the shell. Therefore, the real effects of asymmetric lapping on the frequency mismatch might be larger than predicted. The other reason might be the large original frequency mismatches of the two shells tested, which are 105Hz and 202Hz for the two shells tested. The large frequency mismatch causes the shape of the shell to deviate from the model, and consequently the error between the model and the experiment might be significant.

IV. Conclusions

An analytical model predicting the frequency of wineglass mode of hemi-toroidal shell was derived for the first time. The predictive frequency of the n=2 wineglass mode shape was within 10% of the finite element results and 20% of the experiment results for thin shells. Predictive model of imperfections during the release was derived and compared to experimental results.

Acknowledgment

Devices were designed and tested in MicroSystems Lab of the University of California, Irvine. Fabrication of the devices was performed in Integrated Nanosystem Research Facility (INRF) of UC Irvine. Authors would like to thank Dr. Leiting Dong for valuable discussions on the mathematical derivations.

References

[1] D. M. Rozelle, "The hemispherical resonator ryro: from wineglass to the planets," *Proc. 19th AAS/AIAA Space Flight Mechanics Meeting*, 2009, pp. 1157-1178.

[2] D. Senkal, M. J. Ahamed, M. H. Asadian, S. Askari. and A. M. Shkel, "Demonstration of 1 Million Q-Factor on Microglassblown Wineglass Resonators With Out-of-Plane Electrostatic Transduction," *IEEE, Journal of Microelectromechanical Systems*, vol. 24 no. 1, 2015, pp. 29-37.

[3] J. Cho, T. Nagourney, A. Darvishian, B. Shiari, J. Woo, and K. Najafi, "Fused silica micro birdbath shell resonators with 1.2 million Q and 43 second decay time constant". *Solid-State Sensors, Actuators, and Microsystems Workshop,* Hilton Head Island, South Carolina, USA, June 8-12, 2014, pp. 103-104.

[4] C. Painter and A. Shkel, "Active structural error suppression in MEMS vibratory rate integrating gyroscopes," *IEEE*, *Sensors Journal,* vol. 3, no. 5, 2003, pp. 595-606.

[5] S.-Y. Choi and J.-H. Kim. "Natural frequency split estimation for inextensional vibration of imperfect hemispherical shell." *Journal of sound and vibration*, vol. 330, no.9, 2011, pp. 2094-2106.

[6] J. W. S. B. Rayleigh, The theory of sound, vol. 2. Macmillan, 1896.

[7] N. Bellomo, B. Lods, R. Revelli, and L. Ridolfi, Generalized collocation methods: solutions to nonlinear problems. Springer Science & Business Media, 1980.